Multiple Small RNAs Modulate Rho-Dependent Termination in the Cyclopropane Fatty Acid Synthase mRNA 5' Untranslated Region

Kristen R. Farley[1], Colleen M. Bianco[2], and Carin K. Vanderpool[1#]

[1]Department of Microbiology, University of Illinois Urbana-Champaign, Urbana, Illinois
[2]Present address: Children's Hospital of Philadelphia, Philadelphia, Pennsylvania

#Address correspondence to Carin Vanderpool, cvanderp@illinois.edu

Abstract

Bacterial small RNAs (sRNAs) have been commonly characterized as regulators of post-transcriptional steps of gene expression including translation and stability of mRNA targets. Previous work revealed that the *Escherichia coli* cyclopropane fatty acid synthase (*cfa*) mRNA is regulated by at least five different sRNAs by a proposed mechanism involving regulated *cfa* mRNA turnover by the RNase E degradosome. However, recent work identified the long 5' untranslated region (UTR) of *cfa* mRNA as a potential target for Rho-dependent transcription termination, leading us to question whether sRNAs might regulate *cfa* gene expression at the level of transcription elongation. In this study we report evidence for premature Rho-dependent termination within the long 5' UTR of *cfa*, and demonstrate that a pyrimidine-only tract within the 5' UTR is required for efficient Rho-dependent regulation of *cfa*. Our data suggest that all of the sequence determinants required for efficient Rho-mediated termination are harbored within the *cfa* long mRNA 5' UTR. Finally, we discovered that both the activating sRNA RydC and repressing sRNA CpxQ regulate *cfa* primarily by modulating Rho-dependent termination of *cfa* transcription, with only a minor effect on RNase E degradosome-dependent turnover of *cfa* mRNA. These results illustrate the versatile mechanisms sRNAs use to regulate target gene expression at transcriptional and post-transcriptional levels and suggest that regulation by sRNAs in long UTRs can involve modulation of transcription elongation.

Introduction

Gene regulation mediated by small RNAs (sRNAs) is a significant regulatory process shared among bacteria, archaea, and eukaryotes to rapidly adjust gene expression and promote changes in cellular physiology (Carvalho Barbosa *et al*, 2020). A large number of sRNAs exert their regulatory effects by base pairing with target RNAs (Adams & Storz, 2020). In bacteria, sRNAs often bind to multiple mRNA targets via short, semi-complementary seed regions that are typically between 6 and 8 nucleotides (nt) in length (Hor *et al*, 2020). In *Escherichia coli* and related bacteria, sRNAs often require the RNA chaperone Hfq for stability and proper mRNA target regulation (Jørgensen *et al*, 2020). Many Hfq-dependent sRNAs base-pair near the ribosome binding site (RBS) on target mRNAs to modulate translation and translational regulation can be coupled to changes in mRNA stability. Some sRNAs have been shown to directly modulate mRNA stability by base pairing with ribonuclease E (RNase E) cleavage sites to block mRNA degradation (Jørgensen *et al.*, 2020; Papenfort & Vanderpool, 2015). RNase E is an essential ribonuclease that is responsible for tRNA and rRNA processing, bulk cellular mRNA degradation, and sRNA stability (Cohen & McDowall, 1997). Hfq-dependent sRNAs frequently modulate RNase E-mediated turnover of their mRNA targets.

Although bacterial sRNAs are best known as post-transcriptional regulators, recent work has revealed that some sRNAs can modulate transcription elongation through interactions in long 5' untranslated regions (5' UTRs) of mRNA targets (Bossi *et al*, 2020; Sedlyarova *et al*, 2016). About 25% of *E. coli* mRNAs possess 5' UTRs longer than 80 nt and the levels of approximately half of these long-UTR-mRNAs are altered by bicyclomycin (BCM), an inhibitor of transcription termination factor Rho (Sedlyarova *et al.*, 2016). These observations suggest that Rho-dependent termination events in long 5' UTRs may be common and that there may be more examples of sRNAs that regulate target mRNAs by modulating transcription elongation.

Rho is a ring-shaped, hexameric protein that functions as an essential transcription termination factor in most sequenced bacteria (Boudvillain *et al*, 2013). Rho binds to nascent RNAs at sequences called Rho utilization (*rut*) sites and hydrolyzes ATP to translocate toward RNA polymerase (RNAP) and the transcription elongation complex. Rho destabilizes the elongation complex, leading to transcription termination (Boudvillain *et al.*, 2013). Active translation shields mRNAs from Rho-dependent transcription termination within coding sequences but circumstances that result in the uncoupling of transcription and translation can leave nascent mRNAs susceptible to ribonuclease-mediated degradation and premature Rho-dependent termination (Boudvillain *et al.*, 2013). For example, the sRNA ChiX base pairs with the *chiP* RBS and inhibits translation of *chiP*, leading to *chiPQ* mRNA degradation and

premature Rho-dependent transcription termination early in the *chiP* coding sequence (Bossi *et al*, 2012; Figueroa-Bossi *et al*, 2009). While it is evident how sRNA-mediated translational repression can render target mRNAs susceptible to both RNases and Rho, it is unclear how sRNA regulators binding in long 5' UTRs accomplish this in a translation-independent manner (Bossi *et al.*, 2020). The sRNAs DsrA, ArcZ, and RprA were recently found to act as antiterminators that prevent premature Rho-dependent termination within the *rpoS* mRNA long 5' UTR (Sedlyarova *et al.*, 2016). While the mechanism of regulation is unclear, it is hypothesized that these sRNAs inhibit Rho by disrupting Rho binding within the *rpoS* 5' UTR or by acting as roadblocks that impair Rho translocation along the *rpoS* mRNA. The sRNA SraL similarly acts as an antiterminator within the *rho* mRNA, which is known to be autoregulated (Kung *et al*, 1984; Silva *et al*, 2019). While the mechanistic details remain unclear, SraL is thought to function in a translation-independent manner by base pairing with the *rho* long 5' UTR and inducing mRNA structural changes to make a *rut* site inaccessible (Silva *et al.*, 2019).

The *cfa* mRNA in *E. coli* is regulated both positively and negatively by sRNAs that base pair at different sites within a 212-nt 5' UTR (Bianco *et al*, 2019; Fröhlich *et al*, 2013). The *cfa* gene encodes the bacterial cyclopropane fatty acid (CFA) synthase that catalyzes the installation of cyclopropane rings in unsaturated membrane phospholipids to produce cyclopropane fatty acids (Grogan & Cronan, 1997). Under acidic and oxidative stress conditions, CFAs are thought to promote cell survival by stabilizing the cell membrane and reducing membrane permeability (Grogan & Cronan, 1997; Shabala & Ross, 2008). The Hfq-dependent sRNA RydC is a robust activator of *cfa* and was the first sRNA shown to promote CFA synthesis and influence membrane stability in enteric bacteria (Fröhlich *et al.*, 2013), while CpxQ is an Hfq-dependent sRNA (Chao & Vogel, 2016) that represses *cfa* (Bianco *et al.*, 2019). Previous studies suggested that sRNAs regulated *cfa* by a mechanism involving modulation of RNase E-mediated *cfa* mRNA decay (Bianco *et al.*, 2019; Chao *et al*, 2017; Fröhlich *et al.*, 2013). A recent study suggested there is at least one putative site of premature Rho-dependent transcription termination in the 5' region of the *cfa* CDS (Adams *et al*, 2021), prompting us to further investigate whether sRNA-mediated regulation also affects Rho-dependent termination in the *cfa* long 5' UTR.

In this study we investigated whether the *cfa* 5' UTR is a target for Rho-dependent termination and whether the sRNAs that regulate *cfa* modulate Rho activity. We found that Rho limits expression of the isoform of *cfa* mRNA that has a 212-nt 5' UTR. The sRNA binding sites within the *cfa* 5' UTR flank a pyrimidine-rich region that has hallmarks of a *rut* site, and we show that this region is critical for Rho-dependent *cfa* regulation. The *cfa*-activating sRNAs ArrS and

RydC and the *cfa*-repressing sRNAs CpxQ and GcvB all require Rho to carry out normal levels of regulation. Our data are consistent with a model where sRNAs primarily act via modulation of Rho-dependent termination and not by control of RNase E-dependent turnover of *cfa* mRNA as previously reported by us and others. This work reveals that sRNAs are not solely post-transcriptional regulators, but instead that many are capable of regulating their mRNA targets in a translation-independent manner at the level of transcription elongation.

Results

Transcription of the long *cfa* mRNA isoform is limited by Rho

The *cfa* gene is transcribed from two different promoters (Wang & Cronan, 1994). A distal σ^{70}-dependent promoter produces an mRNA with a 212-nt 5' UTR (*cfa* long mRNA), while a proximal σ^{S}-dependent promoter produces an mRNA with a 34-nt 5' UTR (*cfa* short mRNA) (Figure 1A). To understand if either short or long *cfa* mRNAs are subject to Rho-dependent transcription termination, we measured β-galactosidase activity of various *cfa*-*lacZ* fusions in the wild-type strain and a *rho*-R66S mutant. The *rho*-R66S allele produces a Rho variant with a mutation in the RNA binding domain that causes a general transcription termination defect (Martinez *et al*, 1996). A previously constructed (King *et al*, 2019) *cfa'-'lacZ* translational fusion (*cfa*-Long) encodes the 212-nt 5' UTR of *cfa*, while the *cfa'-'lacZ*-Short (*cfa*-Short) translational fusion has the 34-nt 5' UTR normally produced by transcription from the proximal promoter (Figure 1B). Both fusions extend to the +320 position of the *cfa* coding sequence (CDS) which is linked to the 9th codon of the *lacZ* CDS (Figure 1B). The activity of the *cfa*-Short fusion was similar in both wild-type and *rho*-R66S backgrounds, whereas activity of the *cfa*-Long fusion was significantly higher in the *rho*-R66S mutant (Figure 1B). As a control, we tested the activity of a *rho*'-'*lacZ* fusion in both backgrounds since Rho autoregulates its own transcription via termination within its 5' UTR (Matsumoto *et al*, 1986). Activity of the *rho* fusion was significantly higher in the *rho*-R66S mutant compared to the wild-type strain (Figure S1), indicating that the *rho*-R66S mutation has the expected effect on a known target of Rho-dependent termination. Together these data suggest that sequences within the long 5' UTR of *cfa* mRNA make it susceptible to premature Rho-dependent termination.

A recent study revealed extensive gene regulation by premature Rho-dependent termination across the *E. coli* transcriptome (Adams *et al.*, 2021). RNA 3' end mapping identified a *cfa* RNA with a 3' end corresponding to position +59 of the *cfa* long 5' UTR relative to the σ^{70}-dependent transcription start site (TSS) (+1) (Adams *et al.*, 2021). Since previous work showed that *cfa* mRNA is subject to RNase E-mediated degradation (Chao *et al.*, 2017), the production

of this 3' end could be a result of Rho-dependent transcription termination, processing, or both. In addition to detection of a *cfa* 3' end at position +59, an additional 3' end corresponding to position +330 within the *cfa* CDS (relative to the σ^{70}-dependent TSS) was identified only when cells were grown to stationary phase in LB medium (Adams *et al.*, 2021). In the same study, direct RNA-seq on transcripts isolated from cells grown in the presence or absence of the Rho inhibitor bicyclomycin (BCM) revealed a putative Rho-dependent termination site near position +446 in the *cfa* CDS (Adams *et al.*, 2021). Based on this previous work and our observations (Figure 1B), we hypothesized that Rho binds to a *rut* site located within the *cfa* long 5' UTR and subsequently terminates *cfa* transcription at one or more sites within the 5' UTR or early in the *cfa* CDS. To further assess termination occuring early within the *cfa* CDS, we constructed additional *cfa*'-'*lacZ* fusions that extend to position +800 of the *cfa* CDS (which would include the 3' ends identified in previous studies) and named them *cfa*-Long2 and *cfa*-Short2 (Figure 1C). When we tested the activity of these fusions in the wild-type and *rho*-R66S mutant, we observed that activity of the *cfa*-Short2 fusion is similar in both strains, while activity of the *cfa*-Long2 fusion is significantly higher in the *rho*-R66S mutant (Figure 2C), similar to our results with the original fusions. While the basal activity levels of both extended fusions are lower than the original fusions, the fold-change in activity in wild-type compared to *rho*-R66S for the *cfa*-Long2 fusion is higher compared to the *cfa*-Long fusion (compare Figures 1B and 1C).

Because β-galactosidase production from *cfa*'-'*lacZ* translational fusions is dependent on both *cfa* transcription elongation and translation, we constructed transcriptional fusions to more directly measure the impact of Rho on *cfa* transcription elongation. The *cfa*'-*lacZ*-Long and -Short transcriptional fusions contain the same length UTRs as the translational fusions and both fusions extend to the +320 position of the *cfa* coding sequence (Figure 1D). β-galactosidase activity of the *cfa*-Short transcriptional fusion was similar between the wild-type and *rho*-R66S mutant strains, while activity of the *cfa*-Long transcriptional fusion was significantly higher in the *rho*-R66S mutant (Figure 1D). Since both transcriptional and translational fusions respond similarly to Rho, and we have thoroughly characterized the responses of translational fusions to different sRNAs (Bianco *et al.*, 2019), we carried on using translational fusions and their derivatives unless otherwise stated. Collectively, these results are consistent with the interpretation that Rho-dependent termination requires sequences in the long 5' UTR and that termination efficiency is increased by inclusion of more of the *cfa* coding sequence in reporter constructs.

A pyrimidine-only tract in the *cfa* mRNA long 5' UTR is required for Rho-dependent regulation

Although *rut* sites are not characterized by a specific consensus sequence, they are generally C-rich/G-poor sequences located in unstructured regions of nascent RNA transcripts (Bossi *et al.*, 2020). In some cases, *rut* sites have been found to contain pyrimidine-only tracts (also known as CU-only tracts) that promote Rho-dependent transcription termination (Bossi *et al.*, 2012). We identified a 16-nt CU-only tract at positions +86 to +101 of the *cfa* long 5' UTR. We hypothesized that this tract is part of a *rut* site in the *cfa* 5' UTR and important for Rho-dependent regulation. To test this hypothesis, we measured activity of *cfa*-Long fusion variants with substitutions that convert the sequence from C-rich to G-rich. We found that one C to G substitution (G fusion, Figure 2) had a minimal impact on Rho-dependent regulation compared to the wild-type fusion. Conversely, three C to G substitutions (GGG, Figure 2) resulted in strongly increased activity in the *rho*$^+$ strain background, suggesting the GGG variant is less sensitive to Rho-dependent termination. Six C to G substitutions (GGGGGG, Figure 2), resulted in a further increase in fusion activity in the *rho*$^+$ strain compared to the wild-type fusion control, and activity of this fusion was not increased in the *rho*-R66S compared to the *rho*$^+$ background. This result suggests that Rho can no longer target the GGGGGG variant for premature transcription termination. Together these data suggest that the conversion of the 16-nt CU-only tract within the *cfa* long 5' UTR to a G-rich sequence disrupts Rho's ability to target the mRNA for premature transcription termination, suggesting this sequence is part of a larger *rut* site.

To understand if the putative *rut* site in *cfa* mRNA is conserved, we aligned *cfa* 5' UTR sequences from 10 different bacterial species belonging to the Enterobacteriaceae (Figure S2A). While the CU-only tract is identical between *E. coli*, *Escherichia albertii*, and *Shigella boydii*, it is not conserved among the remaining species (Figure S2A). Since the *cfa* gene in *S. enterica* is regulated by some of the same factors as the *E. coli cfa* gene, including RNase E and RydC (Chao *et al.*, 2017; Fröhlich *et al.*, 2013), we wanted to test whether the *S. enterica cfa* mRNA is also subject to Rho-dependent regulation despite the lack of CU-only tract conservation between *E. coli* and *S. enterica*. To address this hypothesis, we tested the β-galactosidase activity of *S. enterica cfa*-Long and *cfa*-Short translational fusions (*Stm* fusions, Figure S2B) in the *E. coli* wild-type and *rho*-R66S mutant strains (Figure S2B). Analogous to our results with *E. coli cfa* translational fusions, activity of the *Stm cfa*-Short fusion is similar between wild-type and *rho*-R66S mutant backgrounds, while activity of the *Stm cfa*-Long fusion is higher in the *rho*-R66S mutant compared to the wild-type strain (Figure S2B). These data suggest that the *cfa* long mRNA isoform is a common target for premature Rho-dependent

transcription termination in enteric bacteria, although the specific sequences required for Rho binding and subsequent transcription termination may differ between species.

To further characterize the region required for Rho-dependent termination, we measured the activity of *cfa*-Long transcriptional fusion variants that were truncated from the 3' end of the 5' UTR sequence (Figure 3). While basal activities of the fusions vary, fusions containing the 5' UTR to position +138 or greater all display more than 2-fold higher levels of activity in the *rho*-R66S background compared to wild-type (Figure 3). Shorter fusions (+58, +78, +98, +118) show little or no Rho-dependence (Figure 3). The CU-only tract of the 5' UTR is located between positions +85 and +102 (Figure 4A). These data indicate that in addition to the CU-only tract, sequences downstream are also required for efficient Rho-dependent termination in the *cfa* 5' UTR.

Activating and repressing sRNAs modulate Rho-dependent regulation in the *cfa* 5' UTR

The long *cfa* mRNA isoform is regulated by multiple Hfq-dependent sRNAs. RydC, ArrS, and OxyS activate *cfa*, while CpxQ and GcvB repress *cfa* (Bianco *et al.*, 2019). RydC and ArrS bind to overlapping sites in the *cfa* long 5' UTR and previous work suggested that RydC or ArrS base pairing occludes an RNase E cleavage site and impairs the RNase E-mediated degradation of *cfa* mRNA (Bianco *et al.*, 2019; Chao *et al.*, 2017; Fröhlich *et al.*, 2013). Conversely, CpxQ binds upstream of the RydC binding site and we reported that CpxQ also regulates *cfa* by a mechanism requiring the same RNase E cleavage site within the *cfa* long 5' UTR (Bianco *et al.*, 2019). RydC and ArrS bind immediately downstream of the CU-only tract that is critical for Rho-dependent regulation of *cfa*, while CpxQ binds directly upstream of this sequence (Figure 4A). We hypothesized that in addition to modulating RNase E-mediated degradation, RydC/ArrS and CpxQ play an additional regulatory role in modulating premature Rho-dependent termination of *cfa* transcription.

We measured activity of the *cfa*-Long fusion in wild-type (*rho*$^+$) and *rho*-R66S mutant strains carrying a vector control or sRNA-producing plasmid (Figure 4B). We showed previously that sRNAs do not act on the *cfa*-Short fusion (Bianco *et al.*, 2019). RydC and ArrS robustly activate *cfa*-Long fusion activity in the wild-type strain, while CpxQ represses it. In the *rho*-R66S mutant, the magnitude of RydC-dependent activation of *cfa* is greatly diminished, while both ArrS-dependent activation and CpxQ-dependent repression are completely abolished in this background (Figure 4B). Northern blot analysis showed that RydC and CpxQ levels are equivalent in wild-type and *rho*-R66S mutant backgrounds (Figure S3), so the loss of regulation by these sRNAs cannot be attributed to indirect effects on sRNA levels. We observed the same

patterns of sRNA- and Rho-dependent regulation for the *cfa*-Long2 translational fusion and *cfa*-Long transcriptional fusion (Figure S4).

We showed previously that OxyS modestly activates the *cfa*-Long fusion (Bianco *et al.*, 2019) and the predicted OxyS binding site lies far upstream of the CU-only tract near the 5' end of the mRNA (Figure 4A). OxyS-mediated activation is only slightly diminished in the *rho*-R66S mutant strain compared to the wild-type strain (Figure 4B). These data suggest that OxyS may have a modest impact on Rho-dependent regulation of *cfa*, but that it primarily uses a distinct mechanism to activate *cfa* compared to the other sRNAs. GcvB modestly represses the *cfa*-Long fusion and binds at a site that is slightly upstream of the CpxQ binding site (Bianco *et al.*, 2019) (Figure 4A). GcvB-mediated repression is abolished in the *rho*-R66S mutant strain (Figure 4B). These findings suggest that CpxQ and GcvB repress *cfa* by promoting premature Rho-dependent termination via similar mechanisms. In total our results suggest that RydC and ArrS strongly impair Rho-dependent termination to activate *cfa*, while CpxQ and GcvB enhance Rho-dependent termination to repress *cfa*. For the remaining experiments, we focus on further characterization of RydC and CpxQ.

RydC base pairs immediately downstream of the CU-only tract, while CpxQ base-pairs immediately upstream of this sequence (Figure 4A). To understand if sRNA base-pairing at these sites is sufficient to modulate Rho-dependent regulation of *cfa*, we swapped the seed regions that are used for base pairing by each sRNA to generate “seed-swapped” sRNA variants. The variant RydC_CpxQ seed contains the CpxQ seed region sequence in place of the original RydC seed region, and vice versa for the variant CpxQ_RydC seed. We hypothesized that if base pairing upstream or downstream from the CU-only tract is sufficient for repression and activation, respectively, then the variant sRNAs should regulate in accordance with seed pairing. We measured activity of the *cfa*-Long fusion in wild-type and *rho*-R66S mutant strains carrying the vector control or plasmids producing the following sRNAs: RydC, CpxQ_RydC seed, CpxQ, or RydC_CpxQ seed (Figure S5). Regulation by CpxQ and the RydC_CpxQ seed variant was identical; both sRNAs repressed activity of the *cfa*-Long fusion, and this repression was abolished in the *rho*-R66S mutant (Figure S5). In the wild-type strain, RydC activates *cfa* by approximately 15-fold whereas the CpxQ_RydC seed variant activates by approximately 8-fold (Figure S5). In the *rho*-R66S background, both RydC and the CpxQ_RydC seed variant activate *cfa* by only about 2-fold (Figure S5). These results suggest that base pairing either upstream or downstream of the CU-only tract is sufficient for strong repression and activation of *cfa,* respectively, through a mechanism that is Rho-dependent.

RydC and CpxQ impact *cfa* transcription elongation

To examine the roles of RydC and CpxQ in modulating premature termination *in vivo*, we used RT-qPCR to measure the relative steady-state levels of different portions of the *cfa* mRNA in Δ*rydC* Δ*cpxQ* mutant cells expressing either RydC or CpxQ. The relative levels of three different regions of the *cfa* mRNA were measured including the *cfa* long 5' UTR (5' UTR), the 5' portion of the *cfa* CDS (5' CDS), and the 3' portion of the *cfa* CDS (CDS). Figure 5A illustrates predictions for how ratios of the different *cfa* mRNA regions would change with increased or decreased frequencies of termination. At baseline (no sRNAs) we expect the pool of *cfa* mRNAs to be comprised of both full-length and prematurely terminated transcripts (Figure 5A, top panel). When Rho-mediated termination is suppressed (Figure 5A, middle panel), ratios of 5' UTR:CDS and 5' CDS:CDS should decrease relative to the control condition. Conversely, if Rho-mediated termination is enhanced, ratios of 5' UTR:CDS and 5' CDS:CDS should increase relative to the control condition (Figure 5A, bottom panel).

When RydC was produced, the *cfa* 5' UTR:CDS ratio was slightly decreased, and the *cfa* 5' CDS:CDS ratio was significantly decreased relative to the control (Figure 5B), consistent with the expectation that RydC inhibits premature termination to promote higher levels of full-length *cfa* mRNA. The data suggest that RydC promotes elongation past the 5' region of the CDS and into the 3' region of the *cfa* CDS. Conversely, in CpxQ-producing cells, the *cfa* 5' UTR:CDS ratio is increased, consistent with a CpxQ-mediated increase in termination (Figure 5B). There is no significant change in 5' CDS:CDS ratios compared to the control in CpxQ-producing cells. These data suggest that CpxQ primarily modulates a termination event that occurs between the regions detected by the 5' UTR and 5' CDS probes. Together, these data support the model that CpxQ and RydC sRNAs modulate termination within the 5' UTR and early CDS of *cfa* mRNA.

Interplay between Rho and RNase E degradosome in regulation of *cfa*

Previous studies examining sRNA-dependent regulation of *cfa* in *S. enterica* and *E. coli* suggested that *cfa* mRNA is subject to degradation by RNase E due to the presence of an RNase E cleavage site within the *cfa* 5' UTR (Chao *et al.*, 2017; Fröhlich *et al.*, 2013). Recent biochemical and genetic data further suggest that RydC and CpxQ play roles in either inhibiting or enhancing, respectively, the RNase E-mediated degradation of *cfa* mRNA (Bianco *et al.*, 2019). To better understand the combined contributions of RNase E and Rho to the regulation of *cfa*, we examined activity of the *cfa*-Long fusion in a *rho*-R66S *rne131* double mutant strain (Figure 6). The *rne131* allele encodes an RNase E variant that lacks the region for degradosome assembly but retains its ribonucleolytic activity (Lopez *et al*, 1999). Most sRNA-

dependent regulatory effects that act through RNase E require the degradosome (Bobrovskyy & Vanderpool, 2016; Caron *et al*, 2010; Rice *et al*, 2012). We observed that *cfa* fusion activity is similar in the wild-type strain and the *rne131* mutant. Moreover, fusion activity is approximately 3-fold higher in the *rho*-R66S mutant compared to wild-type and the addition of the *rne131* allele to the *rho*-R66S background does not increase the activity further (Figure 6A). These results suggest that premature Rho-dependent transcription termination, and not degradosome-mediated degradation, is primarily responsible for low basal expression of the *cfa*-Long fusion.

To interrogate the possible dual roles of RydC and CpxQ in modulating degradosome- and Rho-mediated regulation of *cfa*, we measured activity of the *cfa*-Long fusion in strains with degradosome and *rho* mutations with and without sRNA production (Figure 6B). RydC and CpxQ regulate the *cfa*-Long fusion similarly in the wild-type strain and *rne131* single mutant background (Figure 6B), suggesting that neither sRNA is acting primarily through altering degradosome activity on *cfa* mRNA. In the *rho*-R66S background, CpxQ-dependent repression and RydC-dependent activation are both diminished and there is no substantial difference in sRNA-mediated regulation between *rho*-R66S mutant and *rho*-R66S *rne131* double mutant strains (Figure 6B). These results suggest that RydC and CpxQ primarily regulate *cfa* by modulating premature Rho-dependent transcription termination and not by antagonizing degradosome activity.

Previous work demonstrated that *Salmonella cfa* mRNA is subject to RNase E-mediated cleavage within the 5' UTR at a site immediately adjacent to the RydC binding site (Chao *et al.*, 2017). Mutation of this cleavage site increased *cfa* mRNA levels and made *cfa* less sensitive to RydC-mediated regulation (Fröhlich *et al.*, 2013). We made a similar mutation in the *E. coli cfa* 5' UTR (GG↓A<u>UUA</u>U to GG↓A<u>GGG</u>U) and showed that the mutation increased *cfa* fusion activity and diminished regulation by RydC and CpxQ (Bianco *et al.*, 2019). Our interpretation at the time was that this mutation inhibited RNase E-mediated degradation and therefore both RydC and CpxQ were acting to modulate RNase E activity on *cfa* mRNA. However, in light of our results in this study, we hypothesized that the mutation (where UUA is replaced by GGG, which we will call G3 here) might impair Rho-dependent regulation of *cfa*. To test this, we compared activity of wild-type *cfa*-Long and *cfa*-LongG3 fusions in the *rho*$^+$ and *rho*-R66S backgrounds carrying an empty vector or RydC- or CpxQ-producing plasmids (Figure 6C). As shown previously, the G3 mutation strongly increases basal levels of *cfa* expression and RydC- and CpxQ-mediated regulation is lost or diminished, respectively (Figure 6C). Mutation of *rho* (*rho*-R66S background) has no impact on the activity of the *cfa*-LongG3 fusion (Figure 6C). These data indeed suggest that the G3 mutation disrupts Rho-dependent regulation of *cfa*, and

that this effect could explain the loss of RydC- and CpxQ-mediated regulation of the G3 fusion. This result does not rule out an additional role for this site in RNase E-mediated cleavage, but leaves the role of RNase E-mediated degradation of *cfa* mRNA unclear.

RydC regulates *cfa* even when RNase E is inactivated

To more directly probe the role of RNase E-mediated degradation in regulating *cfa* mRNA levels in *E. coli*, and the putative role of RydC in protecting the mRNA from this degradation, we used Northern blot analysis. We examined *cfa* mRNA levels in wild-type (*rne*$^+$) and *rne131* mutant strains carrying empty vector or RydC-producing plasmids. In the *rne*$^+$ strain with the vector control, *cfa* mRNA was undetectable, and levels increased substantially in the strain producing RydC (Figure 7A). In the *rne131* degradosome mutant, *cfa* mRNA levels were low but detectable and RydC still substantially increased *cfa* mRNA levels in the in this background (Figure 7A). These results along with the results of reporter fusions (Figure 6B) suggest that the degradosome plays a minor role in *cfa* mRNA turnover and RydC increases *cfa* mRNA levels by a mechanism that is degradosome-independent.

We next compared *cfa* mRNA levels in the wild-type (*rne*$^+$) strain and a mutant strain with a temperature-sensitive RNase E allele (*rne*TS) each carrying either an empty vector or RydC-producing plasmid (Figure 7B). The *rne*TS allele encodes an RNase E variant that is active at the permissive temperature (30°C), but is rapidly inactivated at the non-permissive temperature (44°C) (McDowall *et al*, 1993). In the wild-type strain grown at 30°C, *cfa* mRNA was only detected when RydC was produced (Figure 7B). A faint *cfa* mRNA band was observed in the wild-type strain at 44°C, suggesting that high temperature induces *cfa* mRNA accumulation by an unknown mechanism when RNase E is active. RydC promoted further *cfa* mRNA accumulation at 44°C in the wild-type strain (Figure 7B). In the *rne*Ts strain grown at 30°C (the permissive temperature), *cfa* mRNA was only detected when RydC was produced. Shifting the *rne*TS strain to 44°C resulted in detectable *cfa* mRNA accumulation which was further increased when RydC was produced (Figure 7B). If RydC were activating *cfa* primarily by antagonizing RNase E activity, we would not expect to see RydC-dependent accumulation of *cfa* mRNA at the non-permissive temperature. Taken together, our data suggest that while *cfa* mRNA is subject to RNase E-mediated decay, the sRNAs that activate and repress *cfa* do so primarily by modulating Rho-dependent transcription termination.

Discussion

In this study, we assessed the impact of multiple intersecting regulatory factors including sRNAs, Rho, and RNase E, on control of the cyclopropane fatty acid (*cfa*) synthase mRNA in *E. coli*. Previous studies provided evidence of *cfa* regulation by RNase E and multiple Hfq-dependent sRNAs (Bianco *et al.*, 2019; Chao *et al.*, 2017; Fröhlich *et al.*, 2013). Recent work suggested that the *cfa* long 5' UTR might also be a substrate for premature Rho-dependent transcription termination (Adams *et al.*, 2021). Here, we discover that indeed, transcription of *cfa* is limited by Rho (Figures 1 and S1) and that a CU-rich region in the 5' UTR that likely comprises part of a *rut* site is required for Rho-responsive *cfa* expression (Figure 2). Both activating and repressing sRNAs exert their influence on *cfa* via modulating Rho activity (Figures 4 and S4). The activating sRNA RydC reduces the ratio of truncated to full-length *cfa* transcripts, whereas the repressing sRNA CpxQ increases the same ratio (Figure 5). Despite previous work (including our own) that suggested sRNAs regulate *cfa* by modulating RNase E-dependent turnover of the *cfa* mRNA (Bianco *et al.*, 2019; Chao *et al.*, 2017; Fröhlich *et al.*, 2013), we found here that sRNAs still regulate in a mutant strain where the RNase E degradosome cannot form (Figures 6B and 7A) and in a strain where a temperature-sensitive RNase E is inactivated (Figure 7B). These data are consistent with the model (Figure 8) that the *cfa* mRNA is targeted by Rho for premature transcription termination in the long 5' UTR and that sRNAs, including RydC and CpxQ, regulate transcription elongation by binding directly to the *cfa* 5' UTR and modulating the efficiency of Rho-dependent termination. We hypothesize that sRNAs alter the structure of the *cfa* 5' UTR to enhance (CpxQ) or reduce (RydC) accessibility of the *rut* site.

Transcription termination in bacteria can occur by three mechanisms (Roberts, 2019). Intrinsic (Rho-independent) termination is driven by RNA polymerase (RNAP) interactions with nucleic acids and the structure of nascent RNAs. Rho-dependent termination requires Rho (an ATP-dependent RNA translocase) and an accessible (*i.e.,* single-stranded and not protected by ribosomes) Rho utilization (*rut*) site. Termination by either of these two mechanisms at the ends of open reading frames or operons ensures that only genes that should be co-expressed are transcribed together. A third mechanism of transcription termination depends on the DNA translocase Mfd, and this mechanism primarily aids in removing stalled RNAP from DNA during transcription coupled repair (Adebali *et al*, 2017) and resolution of transcription-replication conflicts (Dutta *et al*, 2011; Trautinger *et al*, 2005). Regulation of bacterial gene expression at the level of transcription is often thought of as occurring mainly at the level of initiation through the actions of transcription factors that modulate the efficiency of RNAP binding. However, regulated transcription termination is a common mode of regulation that controls transcription at

the level of elongation. Both attenuation (increased termination) and antitermination (decreased termination) mechanisms can impact intrinsic and Rho-dependent termination (Turnbough, 2019).

In *E. coli*, 20-30% of transcription termination events are Rho-dependent (Peters *et al*, 2012; Peters *et al*, 2009). Because Rho requires a single-stranded binding site unoccupied by ribosomes, regulators or processes that impact translation or RNA structure can influence the efficiency of Rho-dependent termination. Three different proteins have now been reported to modulate Rho activity and Rho-dependent termination. Hfq – the Sm-like protein known to be involved in sRNA stability and sRNA-mediated regulation, was reported to also bind directly to Rho and to inhibit Rho-dependent termination processes (Rabhi *et al*, 2011). The mechanism of inhibition, and whether it is direct or indirect is not known. Rof, also an Sm-like protein, binds to Rho and inhibits Rho-dependent termination (Gutierrez *et al*, 2007; Pal *et al*, 2019). A recent study used structural, genetic, and biochemical methods to determine that Rof binding to Rho inhibits Rho association with both RNA and RNAP (Said *et al*, 2023). YihE is the third protein factor that has been reported to modulate Rho-dependent termination, and it also binds Rho and inhibits Rho-RNA interactions (Wang *et al*, 2022). What remains a mystery is when and why these regulators act on Rho.

Small RNAs commonly impact translation and structure of mRNA targets, so it follows logically that sRNAs would have the capacity to control Rho-dependent termination and a few examples of this type of regulation have been reported in recent years (Chen *et al*, 2019). The first translation-dependent mechanism of sRNA control of Rho-dependent termination was reported by Bossi and colleagues in 2012 (Bossi *et al.*, 2012). ChiX sRNA represses translation of *chiP* by sequestering the ribosome binding site, which in turn increases the rate of *chiPQ* mRNA turnover (Figueroa-Bossi *et al.*, 2009). Additionally, ChiX-mediated translational repression makes a *rut* site in the *chiP* coding sequence (normally protected by translating ribosomes) more accessible and promotes premature Rho-dependent termination (Bossi *et al.*, 2012), causing a polar effect on *chiQ*. Similarly, the sRNA Spot 42 binds to the *galK* ribosome binding site within the polycistronic *galETKM* mRNA. Repressed translation of *galK* leads to increased Rho-dependent termination within *galK* (Wang *et al*, 2015). Our recent work added to these translation-dependent examples of regulation by demonstrating that sRNAs including SgrS and RyhB that were previously described as post-transcriptional regulators because of their demonstrated ability to repress translation of mRNA targets can also act on some (but not all) targets co-transcriptionally to promote Rho-dependent termination (Reyer *et al*, 2021).

Perhaps even more intriguing are a growing number of examples of sRNAs that modulate Rho-dependent termination by apparently translation-independent mechanisms. Long 5' UTRs are often sites of sRNA action and these sequences are, by definition, untranslated and therefore unprotected by ribosomes. Recent work suggested that at least 250 long 5' UTRs in *E. coli* are targets for Rho-dependent termination (Sedlyarova *et al.*, 2016). Multiple sRNAs have been demonstrated to activate *rpoS* translation by preventing formation of a translation-inhibitory hairpin in the 5' UTR (Battesti *et al*, 2011; Majdalani *et al*, 1998; Majdalani *et al*, 2002; Mandin & Gottesman, 2010). Recently, these sRNAs were also shown to antagonize premature Rho-dependent termination within the 5' UTR (Sedlyarova *et al.*, 2016). In *Salmonella*, SraL base pairs with the 5' UTR of *rho* mRNA to protect it from auto-regulation via Rho-dependent termination (Silva *et al.*, 2019). For both *rpoS* and *rho*, the mechanism of sRNA-mediated interference with Rho-dependent termination within 5' UTRs is unclear. To the best of our knowledge, this work is the first to report an sRNA that mediates increased Rho-dependent termination of its mRNA target. However, the RNA binding protein CsrA promotes Rho-dependent termination by binding to the *pgaA* mRNA 5' UTR and remodeling the secondary structure of the 5' UTR to expose a *rut* site (Figueroa-Bossi *et al*, 2014). We propose that CpxQ binding within the *cfa* 5' UTR is likewise increasing accessibility of the *rut* site to promote Rho-dependent termination and reduced levels of full-length *cfa* mRNA.

Classical examples of sRNA-mediated regulation involve direct translational repression through base-pairing interactions that occlude the translation initiation region (De Lay *et al*, 2013). sRNA-mRNA interactions that occur within a window of approximately 40 nt around the start codon can directly inhibit ribosome binding (Bouvier *et al*, 2008). We now know that sRNAs can also carry out translational regulation of mRNA targets by base pairing at sites that are long distances from translation initiation regions. We and others have described translational repression mechanisms involving sRNA sequestration of translational enhancer sequences (Azam & Vanderpool, 2020; Sharma *et al*, 2007; Yang *et al*, 2014) and ribosome standby sites (Darfeuille *et al*, 2007) in long 5' UTRs. Small RNAs can act as indirect translational repressors by binding upstream (Desnoyers & Masse, 2012) or downstream (Azam & Vanderpool, 2018) of the translation initiation region and recruiting Hfq to bind at sites overlapping the RBS. Perhaps not surprisingly, regulatory mechanisms that act at steps of gene expression other than translation also involve sRNA-mRNA interactions at sites far from the mRNA translation initiation region. Control of mRNA decay can be modulated by sRNAs binding within 5' or 3' UTRs of coding regions (Fröhlich *et al*, 2012; Papenfort *et al*, 2013; Pfeiffer *et al*, 2009). We can now definitively add transcription elongation to the list of molecular processes that sRNAs can

modulate by base pairing at sites distal to the translation initiation region. More work will be required to reveal the molecular mechanisms governing sRNA-dependent modulation of transcription elongation and how sRNAs and Hfq modulate Rho binding to mRNAs and Rho translocation.

Materials and Methods

Bacterial strains, media, and growth conditions

All bacterial strains and plasmids used in this study are listed in Table S1. All strains used are derivatives of *E. coil* K-12 MG1655. Bacterial growth media were purchased from Research Products International (RPI) as pre-mixed powders or were made with individual medium components purchased from Fisher Scientific. Bacteria were cultured in LB broth or on LB agar plates at 37°C unless otherwise stated. Broth cultures were aerated in a tube roller drum (ThermoScientific). All antibiotics and additional growth medium additives were purchased from Gold Biotechnology (GoldBio), Sigma-Aldrich, or Fisher Scientific unless otherwise stated. When necessary, media were supplemented with final concentrations of the following compounds: 100 µg/ml ampicillin (GoldBio), 25 µg/ml chloramphenicol (GoldBio), 50 µg/ml kanamycin (Fisher Scientific), 10 µg/ml tetracycline (GoldBio), 50 µg/ml bicyclomycin (BCM) (Santa Cruz Biotechnology), L-arabinose (Sigma-Aldrich), 0.1 mM isopropyl-β-D-1-thiogalactopyranoside (IPTG) (GoldBio), and 40 µg/ml 5-bromo-4-chloro-3-indolyl β-D-galactopyranoside (X-gal) (GoldBio).

Molecular methods

All oligonucleotides were purchased from Integrated DNA Technologies (IDT) and are listed in Table S2. All reagents and enzymes used for molecular work were purchased from New England Biolabs unless otherwise specified. All PCR reactions required for plasmid construction and additional genetic constructs used Phusion or Q5 High-Fidelity DNA Polymerases. Plasmids were designed *in silico* using Geneious Prime (v. 2020.1.2) and the NEBuilder Assembly Tool (v. 2.7.1), and plasmids were constructed using the NEBuilder HiFi DNA Assembly Master Mix as recommended by the manufacturer. To construct plasmid pKRF004, HindIII-digested pBRCS12 was assembled with *rydC_cpxQ* seed gBlock. To construct plasmid pKRF005, HindIII-digested pBRCS12 was assembled with *cpxQ_rydC* seed gBlock. Plasmids were verified with restriction enzyme digestion and Sanger DNA sequencing at the UIUC Carver Biotechnology Core Sequencing Facility or Plasmidsaurus long read sequencing (Eugene, OR).

Bacterial strain construction

All transcriptional and translational reporter fusions were constructed using λ Red homologous recombination into strain PM1805 and counterselection against *sacB* as previously described (Mandin & Gottesman, 2009). For *cfa'-lacZ* transcriptional fusion construction, gBlock gene fragments extending to different positions of the *cfa* long 5' UTR or *cfa* CDS were fused to *lacZ* with its own RBS and start codon. For *cfa'-'lacZ* and *rho'-'lacZ* translational fusion construction, PCR amplicons or gBlock gene fragments extending to different positions of the 5' UTR or *cfa* CDS were linked in-frame with the 9th codon of the *lacZ* CDS. All reporter constructs were verified with PCR and Sanger DNA sequencing at the UIUC Carver Biotechnology Center Core Sequencing Facility.

A chloramphenicol resistance gene (*cat*) was inserted in the intergenic region between *flgL* and *rne* via λ Red homologous recombination to link the *rne*-3071 (ts) allele to the *cat* gene (Datsenko & Wanner, 2000). The *rho*-R66S, *rne*-131, *rne*-3071, Δ*cpxQ,* and Δ*rydC* mutations were moved from donor strains to recipient strains via P1 *vir* transduction (Miller, 1972). Plasmid pCP20 encoding FLP recombinase was used to remove antibiotic resistance cassettes from Δ*cpxQ*::kan and Δ*rydC*::kan strains as needed (Datsenko & Wanner, 2000).

β-galactosidase assays

Bacterial strains harboring *lacZ* reporter fusions were cultured at 37°C for 16 hours in TB (tryptone broth) medium with arabinose alone or with arabinose + amplicillin. After 16 hours, bacterial strains were subcultured 1:100 in 5 ml of TB + arabinose or TB + arabinose + ampicillin and grown to early or mid-exponential phase. If sRNA induction was not required, cultures were harvested and assayed at mid-log phase. If sRNA induction was required, 0.1 mM IPTG was added at early exponential phase and cells were cultured at 37°C for 1 hour more before harvesting and assaying at mid-log phase. β-galactosidase assays were carried out with chloroform-permeabilized cells as previously described (Miller, 1972) and data are expressed in Miller Units throughout this manuscript.

RNA extraction

Total RNA was extracted from cells using the hot phenol method as previously described (Aiba *et al*, 1981). 1 ml of bacterial cell culture was mixed with a lysis solution containing SDS, EDTA, sodium acetate, and UltraPure Phenol:Water (3.75:1, v/v) (Invitrogen) in a 2.0-ml RNase-free Microcentrifuge Tube (Invitrogen) at 65ºC, and the mixture was shaken at 65ºC/1400 rpm in a Thermomixer (eppendorf) for 15 minutes. Samples were then spun down at room

temperature/21,300 x g in a tabletop microcentrifuge (eppendorf Centrifuge 5425 R) for 10 minutes and the top (aqueous) layer was transferred to a 2.0-ml 5PRIME Phase Lock Gel Heavy wax tube (Quantabio). 500 µl of Phenol:Chloroform:IAA (25:24:1) (Ambion) was added to the wax tube, and the sample was spun down again at room temperature/21,300 x g in the microcentrifuge. After centrifugation, the top (aqueous) layer was transferred to a 2.0-ml RNase-free tube containing 1.3 ml of absolute (200 proof) ethanol and was placed at -80ºC to precipitate the RNA. The next day, the sample was spun down at 4ºC/14,000 x g in the microcentrifuge for 30 minutes. After this centrifugation step, a visible white pellet was typically seen at the bottom of the tube. The ethanol was then decanted from the tube, and the pellet was allowed to dry before resuspension in 10-40 µl of RNase-free molecular biology-grade water at 65ºC/1400 rpm in a Thermomixer. RNA samples were stored at -80ºC. Prior to northern blot analysis and quantitative reverse transcriptase PCR experiments, RNA samples were subjected to DNase digestion using TURBO DNase (Invitrogen) according to the manufacturer's recommendations except twice the recommended enzyme units (4 U) were added and the reactions were incubated for twice the recommended time (1 hour). After DNase digestion, the samples were purified via phenol-chloroform extraction. In brief, two volumes (100 µl) of RNase-free molecular biology-grade water and 0.2 volumes (30 µl) of sodium acetate were added to each DNase digestion reaction. An equivalent volume (180 µl) of acid phenol:chloroform (pH 4.5) (Ambion) was added and each sample was transferred to a 2.0-ml Phase Lock Gel Heavy wax tube. The top (aqueous) layer was transferred to a 2.0-ml RNase-free tube containing 1 ml of absolute (200 proof) ethanol and was placed at -80ºC to precipitate the RNA. The next day, the sample was spun down at 4ºC/14,000 x g in the microcentrifuge for 30 minutes. After this centrifugation step, a visible white pellet was typically seen at the bottom of the tube. The ethanol was then decanted from the tube, and the pellet was allowed to dry before resuspension in 10-40 µl of RNase-free molecular biology-grade water at 65ºC/1400 rpm in a Thermomixer. RNA samples were stored at -80ºC.RNA concentrations were measured fluorometrically using the Qubit RNA Broad Range (BR) Assay kit.

Northern blot analysis

All probes used were DNA probes (IDT). Each probe was radiolabled at the 5' end with fresh [γ-^{32}P] ATP (Perkin Elmer) using the KinaseMax Kit (Invitrogen) according to the manufacturer's suggestions. Radiolabeled probes were purified using ProbeQuant G-50 Micro Columns (Cytiva) according to the manufacturer's recommendations and were stored at -80ºC until use. For nylon membrane stripping and re-probing, the membrane was incubated with boiling 0.1%

SDS for 10 minutes at room temperature. The membrane was then washed twice with 5 ml of ULTRAhyb Ultrasensitive Hybridization Buffer (Invitrogen) before prehybridization with 10 ml of the same buffer at 42°C for 45 minutes.

For analysis of *cfa* mRNA levels, 20 µg RNA samples were mixed with 1X MOPS buffer, formaldehyde (37%), and formamide (100%) before denaturation at 65°C for 15 minutes. Samples were cooled on ice while gel loading buffer with ethidium bromide was added to each sample. Prepared RNA samples were then loaded into the wells of a 0.8% agarose gel and electrophoresed at 80 V for 2 hours in 1X MOPS buffer. A BrightStar-Plus Positively Charged Nylon Membrane (Invitrogen) was cut to size and soaked in RNase-free water before incubation in 10X sodium saline citrate (SSC) solution for 10 minutes with gentle rocking. A capillary transfer apparatus was set up overnight by assembling components in the following order (bottom to top): glass dish containing 10X SSC with a plastic support, long piece of Whatman 3MM filter paper to serve as the wick, 0.8% agarose gel with wells facing down in contact with the wick, nylon membrane, stack of papertowels, glass or plastic plate balanced with weights on top. The capillary transfer was run overnight. The next morning, the capillary transfer apparatus was disassembled and the nylon membrane was washed in 6X SSC for 5 minutes with gentle rocking before RNAs were UV crosslinked to the membrane. The membrane was placed into a hybridization bottle and was prehybridized with 10 ml ULTRAhyb Ultrasensitive Hybridization Buffer (Invitrogen) at 42°C for 45 minutes in a hybridization oven. After prehybridization, the buffer was discarded and 10 ml of fresh hybridization buffer was added to the bottle. Radiolabeled probe was boiled in 1 ml of hybridization buffer for 2 minutes before addition to the bottle. Probes were allowed to hybridize with the membrane overnight at 42°C in a hybridization oven. The next day, the membrane was washed once with 2X SSC/0.1% SDS, once with 0.1X SSC/0.1% SDS, and once with 0.1X SSC for 15 minutes each wash at 42°C in a hybridization oven. The membrane was then exposed to a phosphorimager screen overnight. Results were visualized using a Typhoon FLA 9500 Phosphorimager (GE).

For analysis of sRNA levels, 10 µg RNA samples were mixed with Gel Loading Buffer II (GLBII) before denaturation at 95°C for 2 minutes. Samples were cooled on ice and loaded into the wells of an 8% Urea-PAGE gel. The gel was electrophoresed at 10 W (constant) in 1X TBE buffer for 30 minutes or until the gel loading dyes reached their desired locations on the gel. RNAs from the gel were transferred to a BrightStar-Plus Positively Charged Nylon Membrane (Invitrogen) using an electrotransfer apparatus (Bio-Rad). The electroblot transfer sandwich was assembled as follows (bottom to top): dark portion of casette, sponge soaked in 0.5X TBE, two pieces of Whatman 3MM paper soaked in 20X SSC, gel, nylon membrane soaked in 20X SSC,

two pieces of Whatman 3MM paper soaked in 20X SSC, sponge soaked in 0.5X TBE, clear portion of cassette. Electrotransfer was run on ice at 250 mA (constant) for 4 hours with pre-chilled 0.5X TBE buffer. After electrotransfer, the electroblot transfer sandwich was disassembled and RNAs were UV crosslinked to the nylon membrane. The membrane was placed into a hybridization bottle and was prehybridized with 5 ml ULTRAhyb Ultrasensitive Hybridization Buffer (Invitrogen) at 42°C for 45 minutes in a hybridization oven. After prehybridization, the buffer was discarded and 5 ml of fresh hybridization buffer was added to the bottle. Radiolabeled probe was boiled in 1 ml of hybridization buffer for 2 minutes before addition to the bottle. Probes were allowed to hybridize with the membrane overnight at 42°C in a hybridization oven. The next day, the membrane was washed once with 2X SSC/0.1% SDS, once with 0.1X SSC/0.1% SDS, and once with 0.1X SSC for 15 minutes each wash at 42°C in a hybridization oven. The membrane was then exposed to a phosphorimager screen overnight. Results were visualized using a Typhoon FLA 9500 Phosphorimager (GE).

Quantitative reverse transcriptase PCR (RT-qPCR)

RNA extracts were treated with TURBO DNase (Invitrogen) to remove contaminating DNA as described above. Each RNA sample was verified to be DNA-free using 40-cycle PCR reactions with each RT-qPCR primer pair. The RNA concentration was then quantified using the Qubit RNA Broad Range (BR) kit. RT-qPCR reactions (10 µl) were set up by mixing 250 ng RNA with the appropriate forward primer, reverse primer, probe, and Luna Probe One-Step RT-qPCR 4X Mix with UDG (NEB) according to the manufacturer's recommendations. Identical no-Reverse-Transcriptase (RT) reactions were set up using Luna Probe One-Step RT-qPCR 4X Mix with UDG that was first heated at 95°C for 5 minutes to inactivate RT. As a further control, no-template reactions were also included. RT-qPCR reactions were run on a Bio-Rad CFX Connect Real-Time System with Bio-Rad CFX Manager (Version 3.1) software in 0.2 ml 96-well PCR plates (dot scientific inc.) sealed with transparent Microseal B Adhesive Sealer (Bio-Rad). Data were analyzed using the comparative Ct ($2^{-\Delta\Delta Ct}$) method.

Acknowledgements

We would like to thank Asma Hatoum-Aslan, Jim Slauch, and members of the Slauch lab for thoughtful discussions and experimental advice throughout this study. We also thank past and present members of the Vanderpool lab for strains, phage, plasmids, advice, and discussions. Special thanks to Rachel Mooney and Robert Landick (U.W. Madison) for strains and plasmids

and advice. This work was supported by the National Institutes of Health R35 grant (R35 GM139557) awarded to C.K.V.

References

Adams PP, Baniulyte G, Esnault C, Chegireddy K, Singh N, Monge M, Dale RK, Storz G, Wade JT (2021) Regulatory roles of Escherichia coli 5' UTR and ORF-internal RNAs detected by 3' end mapping. *Elife* 10

Adams PP, Storz G (2020) Prevalence of small base-pairing RNAs derived from diverse genomic loci. *Biochim Biophys Acta Gene Regul Mech* 1863: 194524

Adebali O, Chiou YY, Hu J, Sancar A, Selby CP (2017) Genome-wide transcription-coupled repair in Escherichia coli is mediated by the Mfd translocase. *Proc Natl Acad Sci U S A* 114: E2116-E2125

Aiba H, Adhya S, de Crombrugghe B (1981) Evidence for two functional gal promoters in intact Escherichia coli cells. *J Biol Chem* 256: 11905-11910

Azam MS, Vanderpool CK (2018) Translational regulation by bacterial small RNAs via an unusual Hfq-dependent mechanism. *Nucleic Acids Res* 46: 2585-2599

Azam MS, Vanderpool CK (2020) Translation inhibition from a distance: The small RNA SgrS silences a ribosomal protein S1-dependent enhancer. *Mol Microbiol* 114: 391-408

Battesti A, Majdalani N, Gottesman S (2011) The RpoS-mediated general stress response in Escherichia coli. *Annu Rev Microbiol* 65: 189-213

Bianco CM, Fröhlich KS, Vanderpool CK (2019) Bacterial Cyclopropane Fatty Acid Synthase mRNA Is Targeted by Activating and Repressing Small RNAs. *J Bacteriol* 201

Bobrovskyy M, Vanderpool CK (2016) Diverse mechanisms of post-transcriptional repression by the small RNA regulator of glucose-phosphate stress. *Mol Microbiol* 99: 254-273

Bossi L, Figueroa-Bossi N, Bouloc P, Boudvillain M (2020) Regulatory interplay between small RNAs and transcription termination factor Rho. *Biochim Biophys Acta Gene Regul Mech* 1863: 194546

Bossi L, Schwartz A, Guillemardet B, Boudvillain M, Figueroa-Bossi N (2012) A role for Rho-dependent polarity in gene regulation by a noncoding small RNA. *Genes Dev* 26: 1864-1873

Boudvillain M, Figueroa-Bossi N, Bossi L (2013) Terminator still moving forward: expanding roles for Rho factor. *Curr Opin Microbiol* 16: 118-124

Bouvier M, Sharma CM, Mika F, Nierhaus KH, Vogel J (2008) Small RNA binding to 5' mRNA coding region inhibits translational initiation. *Mol Cell* 32: 827-837

Caron MP, Lafontaine DA, Masse E (2010) Small RNA-mediated regulation at the level of transcript stability. *RNA Biol* 7: 140-144

Carvalho Barbosa C, Calhoun SH, Wieden HJ (2020) Non-coding RNAs: what are we missing? *Biochem Cell Biol* 98: 23-30

Chao Y, Li L, Girodat D, Forstner KU, Said N, Corcoran C, Smiga M, Papenfort K, Reinhardt R, Wieden HJ *et al* (2017) In Vivo Cleavage Map Illuminates the Central Role of RNase E in Coding and Non-coding RNA Pathways. *Mol Cell* 65: 39-51

Chao Y, Vogel J (2016) A 3' UTR-Derived Small RNA Provides the Regulatory Noncoding Arm of the Inner Membrane Stress Response. *Mol Cell* 61: 352-363

Chen J, Morita T, Gottesman S (2019) Regulation of Transcription Termination of Small RNAs and by Small RNAs: Molecular Mechanisms and Biological Functions. *Front Cell Infect Microbiol* 9: 201

Cohen SN, McDowall KJ (1997) RNase E: still a wonderfully mysterious enzyme. *Mol Microbiol* 23: 1099-1106

Darfeuille F, Unoson C, Vogel J, Wagner EG (2007) An antisense RNA inhibits translation by competing with standby ribosomes. *Mol Cell* 26: 381-392

Datsenko KA, Wanner BL (2000) One-step inactivation of chromosomal genes in Escherichia coli K-12 using PCR products. *Proc Natl Acad Sci U S A* 97: 6640-6645

De Lay N, Schu DJ, Gottesman S (2013) Bacterial small RNA-based negative regulation: Hfq and its accomplices. *J Biol Chem* 288: 7996-8003

Desnoyers G, Masse E (2012) Noncanonical repression of translation initiation through small RNA recruitment of the RNA chaperone Hfq. *Genes Dev* 26: 726-739

Dutta D, Shatalin K, Epshtein V, Gottesman ME, Nudler E (2011) Linking RNA polymerase backtracking to genome instability in E. coli. *Cell* 146: 533-543

Figueroa-Bossi N, Schwartz A, Guillemardet B, D'Heygere F, Bossi L, Boudvillain M (2014) RNA remodeling by bacterial global regulator CsrA promotes Rho-dependent transcription termination. *Genes Dev* 28: 1239-1251

Figueroa-Bossi N, Valentini M, Malleret L, Fiorini F, Bossi L (2009) Caught at its own game: regulatory small RNA inactivated by an inducible transcript mimicking its target. *Genes Dev* 23: 2004-2015

Fröhlich KS, Papenfort K, Berger AA, Vogel J (2012) A conserved RpoS-dependent small RNA controls the synthesis of major porin OmpD. *Nucleic Acids Res* 40: 3623-3640

Fröhlich KS, Papenfort K, Fekete A, Vogel J (2013) A small RNA activates CFA synthase by isoform-specific mRNA stabilization. *EMBO J* 32: 2963-2979

Grogan DW, Cronan JE, Jr. (1997) Cyclopropane ring formation in membrane lipids of bacteria. *Microbiol Mol Biol Rev* 61: 429-441

Gutierrez P, Kozlov G, Gabrielli L, Elias D, Osborne MJ, Gallouzi IE, Gehring K (2007) Solution structure of YaeO, a Rho-specific inhibitor of transcription termination. *J Biol Chem* 282: 23348-23353

Hor J, Matera G, Vogel J, Gottesman S, Storz G (2020) Trans-Acting Small RNAs and Their Effects on Gene Expression in Escherichia coli and Salmonella enterica. *EcoSal Plus* 9

Jørgensen MG, Pettersen JS, Kallipolitis BH (2020) sRNA-mediated control in bacteria: An increasing diversity of regulatory mechanisms. *Biochim Biophys Acta Gene Regul Mech* 1863: 194504

King AM, Vanderpool CK, Degnan PH (2019) sRNA Target Prediction Organizing Tool (SPOT) Integrates Computational and Experimental Data To Facilitate Functional Characterization of Bacterial Small RNAs. *mSphere* 4

Kung H, Bekesi E, Guterman SK, Gray JE, Traub L, Calhoun DH (1984) Autoregulation of the rho gene of Escherichia coli K-12. *Mol Gen Genet* 193: 210-213

Lopez PJ, Marchand I, Joyce SA, Dreyfus M (1999) The C-terminal half of RNase E, which organizes the Escherichia coli degradosome, participates in mRNA degradation but not rRNA processing in vivo. *Mol Microbiol* 33: 188-199

Majdalani N, Cunning C, Sledjeski D, Elliott T, Gottesman S (1998) DsrA RNA regulates translation of RpoS message by an anti-antisense mechanism, independent of its action as an antisilencer of transcription. *Proc Natl Acad Sci U S A* 95: 12462-12467

Majdalani N, Hernandez D, Gottesman S (2002) Regulation and mode of action of the second small RNA activator of RpoS translation, RprA. *Mol Microbiol* 46: 813-826

Mandin P, Gottesman S (2009) A genetic approach for finding small RNAs regulators of genes of interest identifies RybC as regulating the DpiA/DpiB two-component system. *Mol Microbiol* 72: 551-565

Mandin P, Gottesman S (2010) Integrating anaerobic/aerobic sensing and the general stress response through the ArcZ small RNA. *EMBO J* 29: 3094-3107

Martinez A, Opperman T, Richardson JP (1996) Mutational analysis and secondary structure model of the RNP1-like sequence motif of transcription termination factor Rho. *J Mol Biol* 257: 895-908

Matsumoto Y, Shigesada K, Hirano M, Imai M (1986) Autogenous regulation of the gene for transcription termination factor rho in Escherichia coli: localization and function of its attenuators. *J Bacteriol* 166: 945-958

McDowall KJ, Hernandez RG, Lin-Chao S, Cohen SN (1993) The ams-1 and rne-3071 temperature-sensitive mutations in the ams gene are in close proximity to each other and cause substitutions within a domain that resembles a product of the Escherichia coli mre locus. *J Bacteriol* 175: 4245-4249

Miller JH (1972) Experiments in Molecular Genetics. *Cold Spring Harbor Laboratory Press*

Pal K, Yadav M, Jain S, Ghosh B, Sen R, Sen U (2019) Vibrio cholerae YaeO is a Structural Homologue of RNA Chaperone Hfq that Inhibits Rho-dependent Transcription Termination by Dissociating its Hexameric State. *J Mol Biol* 431: 4749-4766

Papenfort K, Sun Y, Miyakoshi M, Vanderpool CK, Vogel J (2013) Small RNA-mediated activation of sugar phosphatase mRNA regulates glucose homeostasis. *Cell* 153: 426-437

Papenfort K, Vanderpool CK (2015) Target activation by regulatory RNAs in bacteria. *FEMS Microbiol Rev* 39: 362-378

Peters JM, Mooney RA, Grass JA, Jessen ED, Tran F, Landick R (2012) Rho and NusG suppress pervasive antisense transcription in Escherichia coli. *Genes Dev* 26: 2621-2633

Peters JM, Mooney RA, Kuan PF, Rowland JL, Keles S, Landick R (2009) Rho directs widespread termination of intragenic and stable RNA transcription. *Proc Natl Acad Sci U S A* 106: 15406-15411

Pfeiffer V, Papenfort K, Lucchini S, Hinton JC, Vogel J (2009) Coding sequence targeting by MicC RNA reveals bacterial mRNA silencing downstream of translational initiation. *Nat Struct Mol Biol* 16: 840-846

Rabhi M, Espeli O, Schwartz A, Cayrol B, Rahmouni AR, Arluison V, Boudvillain M (2011) The Sm-like RNA chaperone Hfq mediates transcription antitermination at Rho-dependent terminators. *EMBO J* 30: 2805-2816

Reyer MA, Chennakesavalu S, Heideman EM, Ma X, Bujnowska M, Hong L, Dinner AR, Vanderpool CK, Fei J (2021) Kinetic modeling reveals additional regulation at co-transcriptional level by post-transcriptional sRNA regulators. *Cell Rep* 36: 109764

Rice JB, Balasubramanian D, Vanderpool CK (2012) Small RNA binding-site multiplicity involved in translational regulation of a polycistronic mRNA. *Proc Natl Acad Sci U S A* 109: E2691-2698

Roberts JW (2019) Mechanisms of Bacterial Transcription Termination. *J Mol Biol* 431: 4030-4039

Said N, Finazzo M, Hilal T, Wang B, Selinger TL, Gjorgjevikj D, Artsimovitch I, Wahl MC (2023) Sm-like protein Rof inhibits transcription termination factor rho by binding site obstruction and conformational insulation. *bioRxiv*

Sedlyarova N, Shamovsky I, Bharati BK, Epshtein V, Chen J, Gottesman S, Schroeder R, Nudler E (2016) sRNA-Mediated Control of Transcription Termination in E. coli. *Cell* 167: 111-121 e113

Shabala L, Ross T (2008) Cyclopropane fatty acids improve Escherichia coli survival in acidified minimal media by reducing membrane permeability to H+ and enhanced ability to extrude H+. *Res Microbiol* 159: 458-461

Sharma CM, Darfeuille F, Plantinga TH, Vogel J (2007) A small RNA regulates multiple ABC transporter mRNAs by targeting C/A-rich elements inside and upstream of ribosome-binding sites. *Genes Dev* 21: 2804-2817

Silva IJ, Barahona S, Eyraud A, Lalaouna D, Figueroa-Bossi N, Masse E, Arraiano CM (2019) SraL sRNA interaction regulates the terminator by preventing premature transcription termination of rho mRNA. *Proc Natl Acad Sci U S A* 116: 3042-3051

Trautinger BW, Jaktaji RP, Rusakova E, Lloyd RG (2005) RNA polymerase modulators and DNA repair activities resolve conflicts between DNA replication and transcription. *Mol Cell* 19: 247-258

Turnbough CL, Jr. (2019) Regulation of Bacterial Gene Expression by Transcription Attenuation. *Microbiol Mol Biol Rev* 83

Wang AY, Cronan JE, Jr. (1994) The growth phase-dependent synthesis of cyclopropane fatty acids in Escherichia coli is the result of an RpoS(KatF)-dependent promoter plus enzyme instability. *Mol Microbiol* 11: 1009-1017

Wang B, Pei H, Lu Z, Xu Y, Han S, Jia Z, Zheng J (2022) YihE is a novel binding partner of Rho and regulates Rho-dependent transcription termination in the Cpx stress response. *iScience* 25: 105483

Wang X, Ji SC, Jeon HJ, Lee Y, Lim HM (2015) Two-level inhibition of galK expression by Spot 42: Degradation of mRNA mK2 and enhanced transcription termination before the galK gene. *Proc Natl Acad Sci U S A* 112: 7581-7586

Yang Q, Figueroa-Bossi N, Bossi L (2014) Translation enhancing ACA motifs and their silencing by a bacterial small regulatory RNA. *PLoS Genet* 10: e1004026

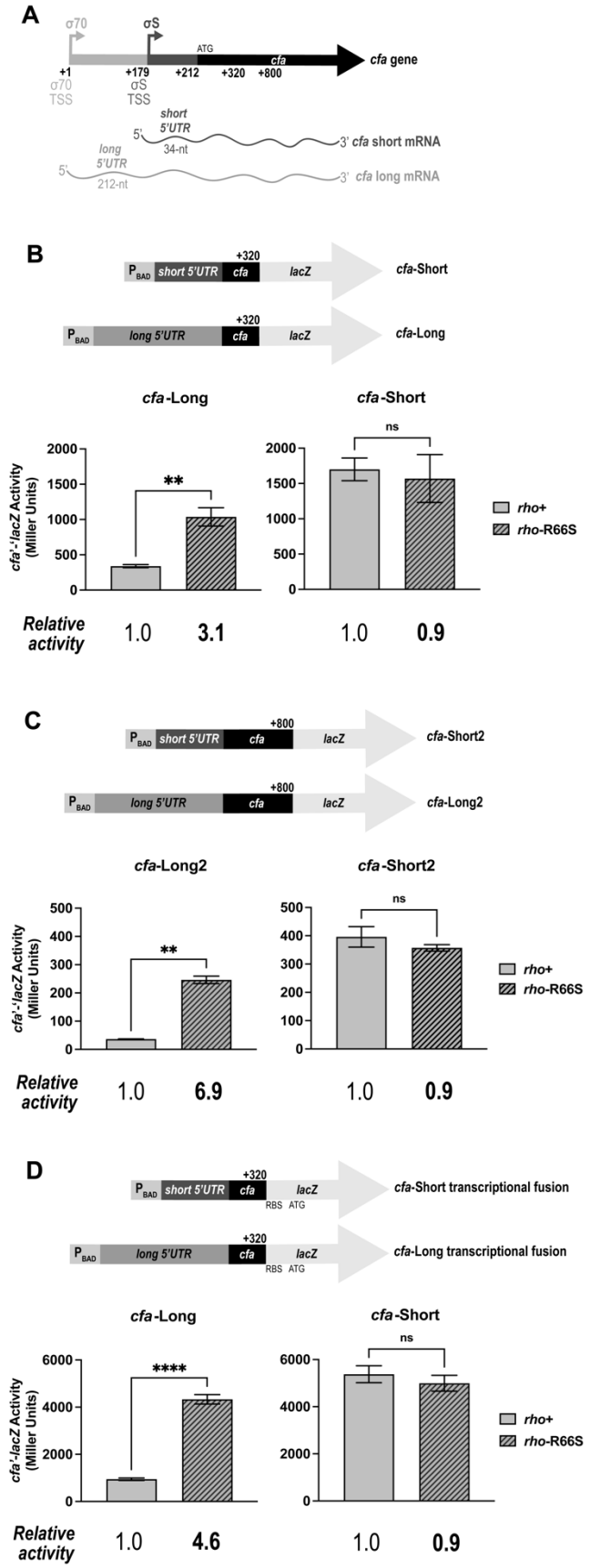

Figure 1. The long 5' UTR of *cfa* mRNA is required for Rho-dependent regulation. A. The long *cfa* mRNA isoform contains a 212-nt 5' UTR (*cfa*-Long), while the short *cfa* mRNA isoform contains a 34-nucleotide 5' UTR (*cfa*-Short). **B.** *cfa*-Long and *cfa*-Short translational fusion constructs contain the respective UTRs and the first 36 codons of the *cfa* coding sequence (up to position +320-nt) fused to the 9th codon of the *lacZ* CDS (top). Both fusions are controlled by an arabinose-inducible promoter (P_{BAD}). β-galactosidase activity of fusion strains was measured at mid-exponential phase. Error bars represent the standard deviations of three biological replicates and statistical significance was determined using two-tailed Welch's t-tests by comparing the fusion activity in the wild-type strain versus the *rho*-R66S mutant (**$P < 0.05$). **C.** *cfa*-Long2 and *cfa*-Short2 fusions contain the same UTR regions with the first 196 codons (up to +800-nt) of the *cfa* CDS fused to the 9th codon of the *lacZ* CDS (top). β-galactosidase activity was measured and data analyzed as described in B. **D.** *cfa*-Long and *cfa*-Short transcriptional fusion constructs contain the same fragments as the corresponding translational fusions in B. β-galactosidase activity was measured and data analyzed as described in B. (****$P < 0.0001$).

CU-only tract	Sequence
WT	...UUCCUCCUUUCCCUCU...
G	...UUCCUCCUUUCCCUGU...
GGG	...UUCCUCCUUUGGGUCU...
GGGGGG	...UUCCUGGUUUGGGUGU...

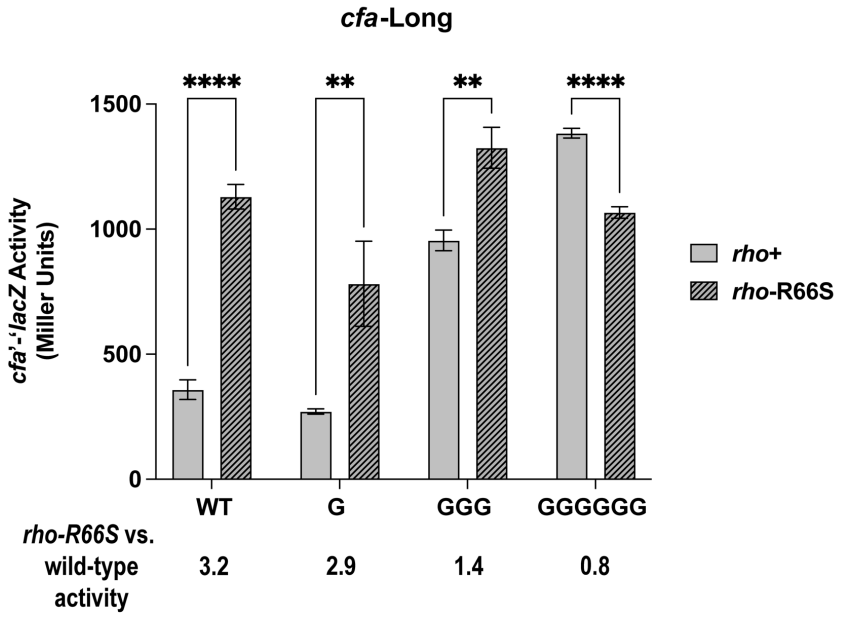

Figure 2. A pyrimidine-only tract in the *cfa* 5' UTR is required for Rho-dependent regulation. The CU-only tract identified within the *cfa* long 5' UTR was converted from a C-rich sequence to a G-rich sequence in the *cfa*-Long translational fusion to generate three variant fusions. Variant fusions have C:G substitutions as shown in red font. The β-galactosidase activity of each fusion was tested in the wild-type or *rho*-R66S mutant strain background. β-galactosidase activity is expressed in Miller Units and the activity was measured at mid-exponential phase. Error bars represent the standard deviations of three biological replicates and statistical significance was determined using multiple unpaired Welch's t-tests by comparing the activity in the wild-type strain versus the *rho*-R66S mutant (****P < 0.001).

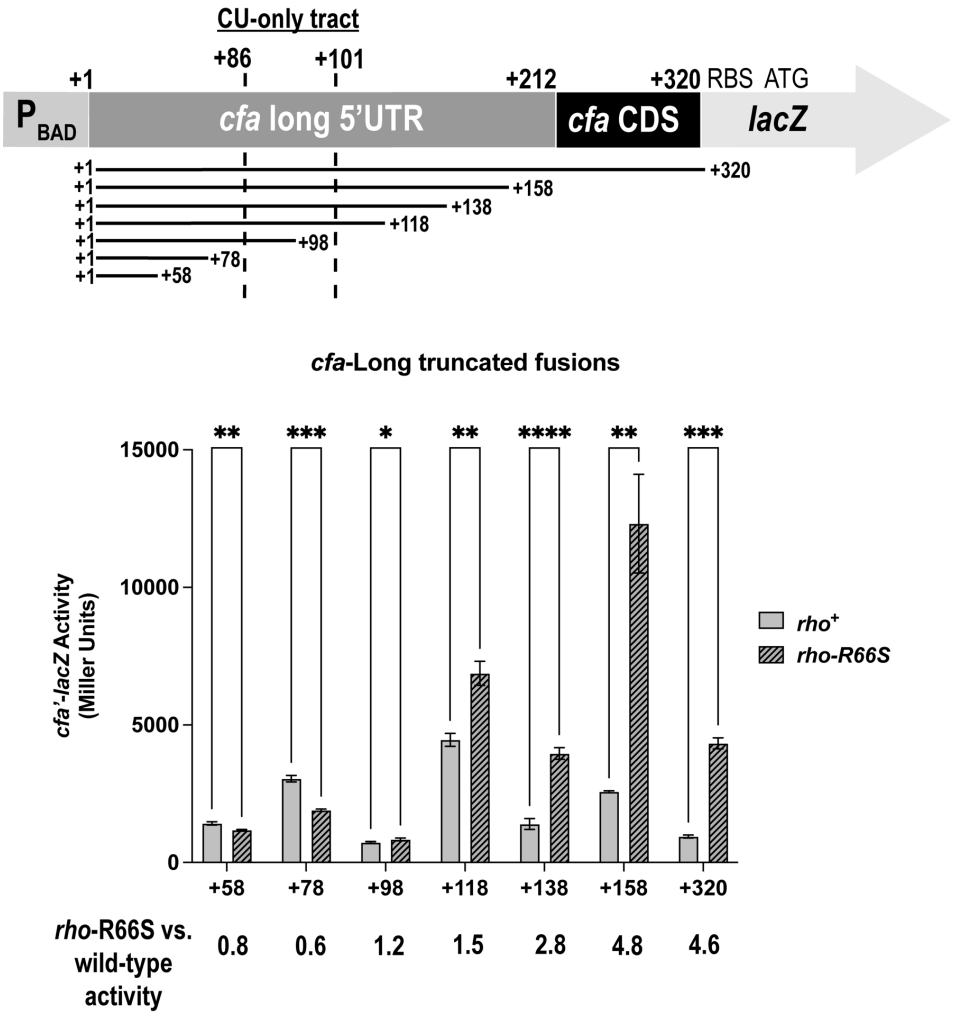

Figure 3. The *cfa* long 5' UTR contains all sequences needed for Rho-dependent regulation. Six *cfa*-Long transcriptional fusions that were truncated from the 3' end were constructed (top). The β-galactosidase activity of each truncated fusion was tested in the wild-type or *rho*-R66S mutant strain background (bottom). β-galactosidase activity is expressed in Miller Units and the activity was measured at mid-exponential phase. Error bars represent the standard deviations of three biological replicates and statistical significance was determined using multiple unpaired Welch's t-tests by comparing the activity in the wild-type strain versus the *rho*-R66S mutant (****P < 0.001).

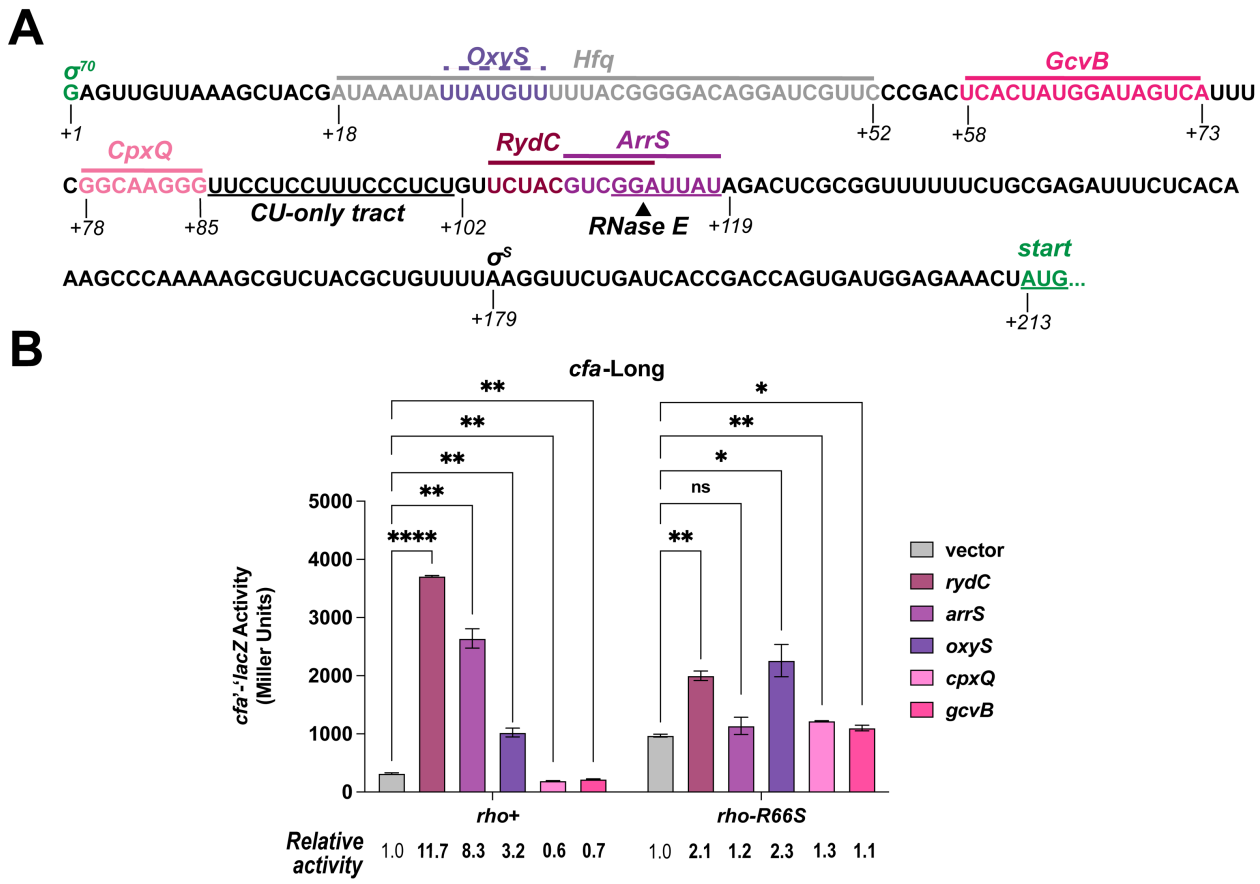

Figure 4. Activating and repressing sRNAs modulate Rho-dependent regulation of *cfa* mRNA. **A.** The sequence of the *cfa* 5' UTR with predicted Hfq and sRNA binding sites. Beginning from the σ^{70}-dependent transcription start site (TSS) position (+1), important binding sites are indicated with solid lines (for validated binding sites) or dotted lines (for predicted sites) above the sequence. The predicted RNase E cleavage site and CU-only tract are underlined. The arrow indicates the predicted RNase E cleavage point. **B.** β-galactosidase activity of the *cfa*-Long translational fusion in the wild-type strain or *rho-R66S* mutant in the presence of an empty vector control or ectopic overexpression of the sRNAs RydC, ArrS, OxyS, CpxQ, or GcvB. β-galactosidase activity is expressed in Miller Units and the activity was measured at mid-exponential phase after one hour of sRNA induction. Error bars represent the standard deviations of three biological replicates and statistical significance was determined using a multiple unpaired Welch's t-tests (****P < 0.001).

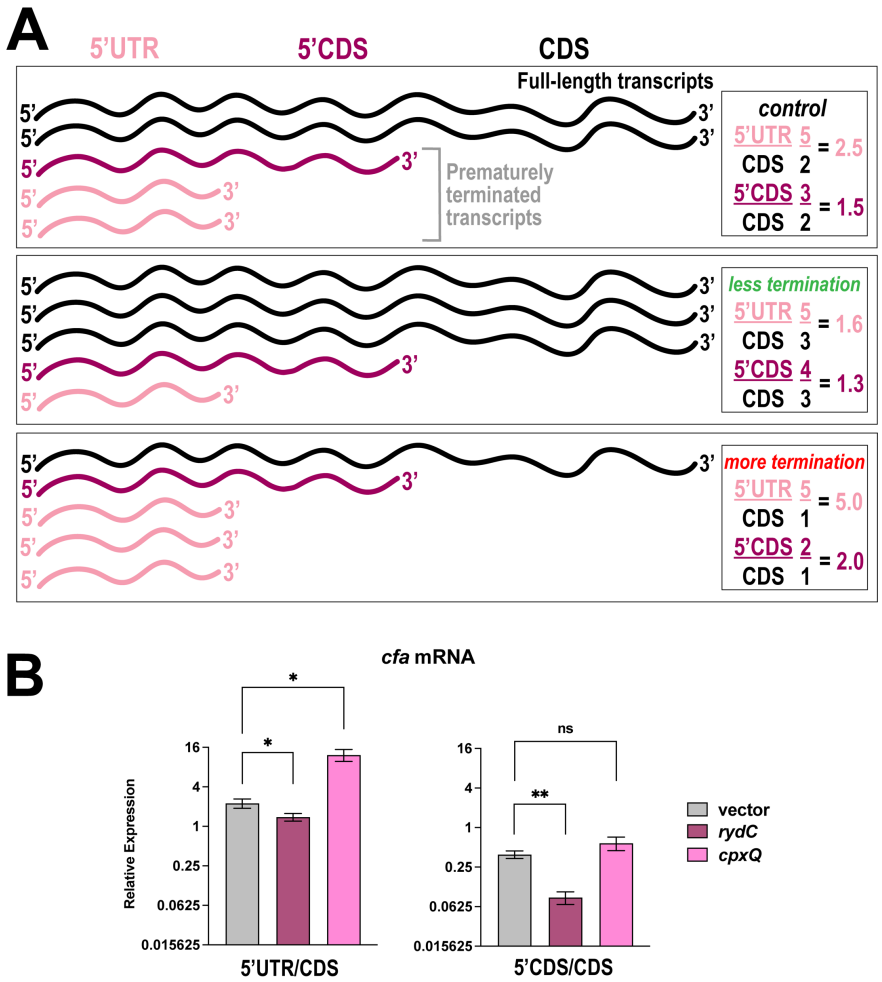

Figure 5. RydC and CpxQ modulate production of full-length *cfa* mRNA. A. Predictions for ratios of different regions of a transcript subject to Rho-dependent termination with increased or decreased efficiency of Rho-dependent termination. **B.** RT-qPCR analysis was used to measure the relative levels of different regions of the *cfa* mRNA in Δ*cpxQ* Δ*rydC* mutant cells containing an empty vector or plasmid expressing either RydC or CpxQ. The relative levels of three different regions of *cfa* mRNA were measured including the long 5' UTR (5' UTR), the 5' portion of the CDS (5' CDS), and the 3' portion of the CDS (CDS). Error bars represent the standard deviations of three biological replicates and statistical significance was determined using multiple unpaired Welch's t-tests (**P < 0.05).

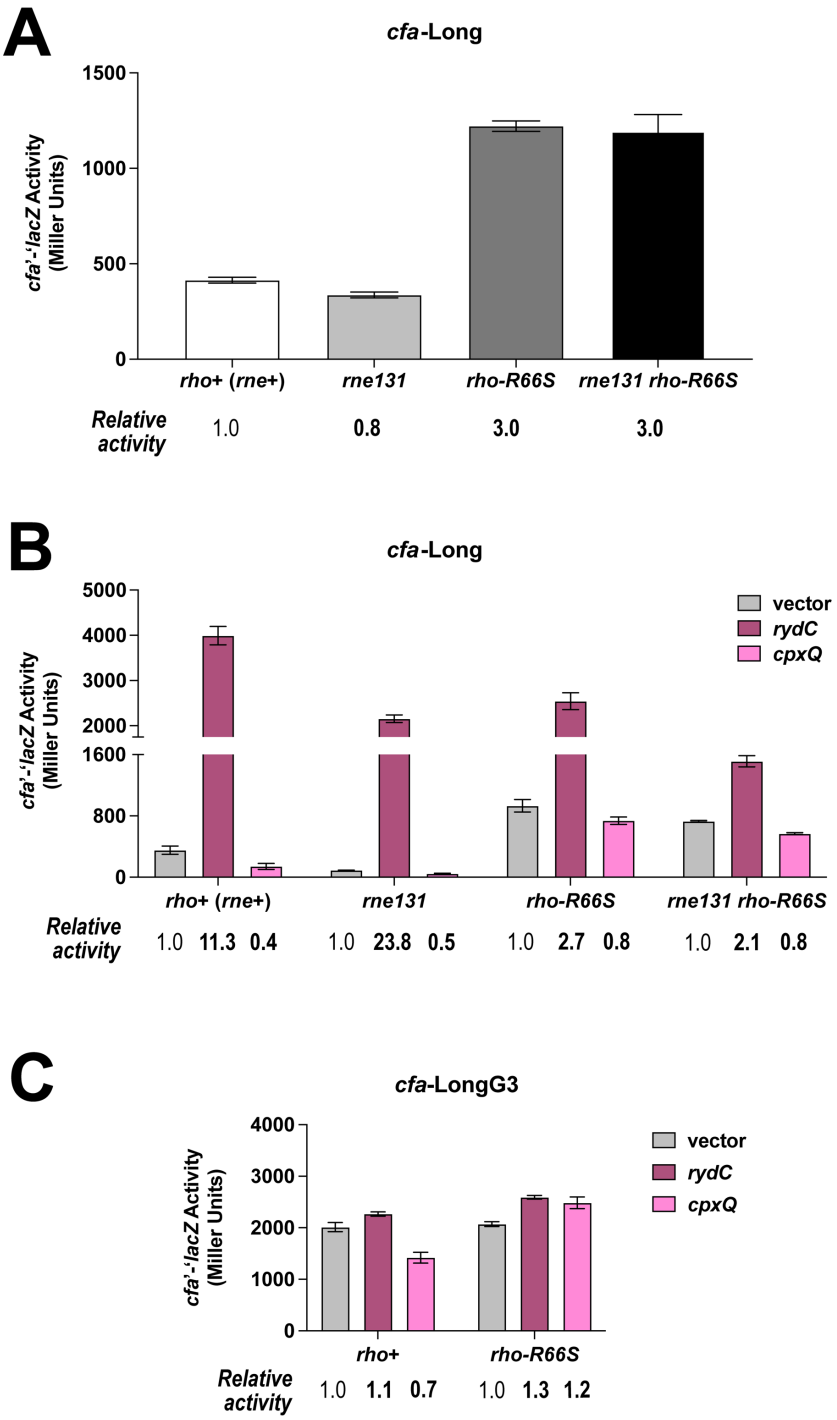

Figure 6. Activating and repressing sRNAs primarily regulate Rho-dependent regulation of *cfa* mRNA. A. β-galactosidase activity of the *cfa*-Long translational fusion in the wild-type, *rne131* mutant, *rho*-R66S mutant, and *rne131 rho*-R66S mutant strains. β-galactosidase activity is expressed in Miller Units and the activity was measured at mid-exponential phase. Error bars

represent the standard deviations of three biological replicates. **B.** β-galactosidase activity of the *cfa* Long translational fusion in the wild-type, *rne131* mutant, *rho*-R66S mutant, and *rne131 rho*-R66S mutant strains in the presence of an empty vector control or plasmid expressing RydC or CpxQ sRNAs. β-galactosidase activity is expressed in Miller Units and the activity was measured at mid-exponential phase after one hour of sRNA induction. Error bars represent the standard deviations of three biological replicates. **C.** β-galactosidase activity of the *cfa*-LongG3 translational fusion in the wild-type strain or *rho*-R66S mutant in presence of an empty vector control (gray bars) or plasmid expressing RydC or CpxQ. Error bars represent the standard deviations of three biological replicates.

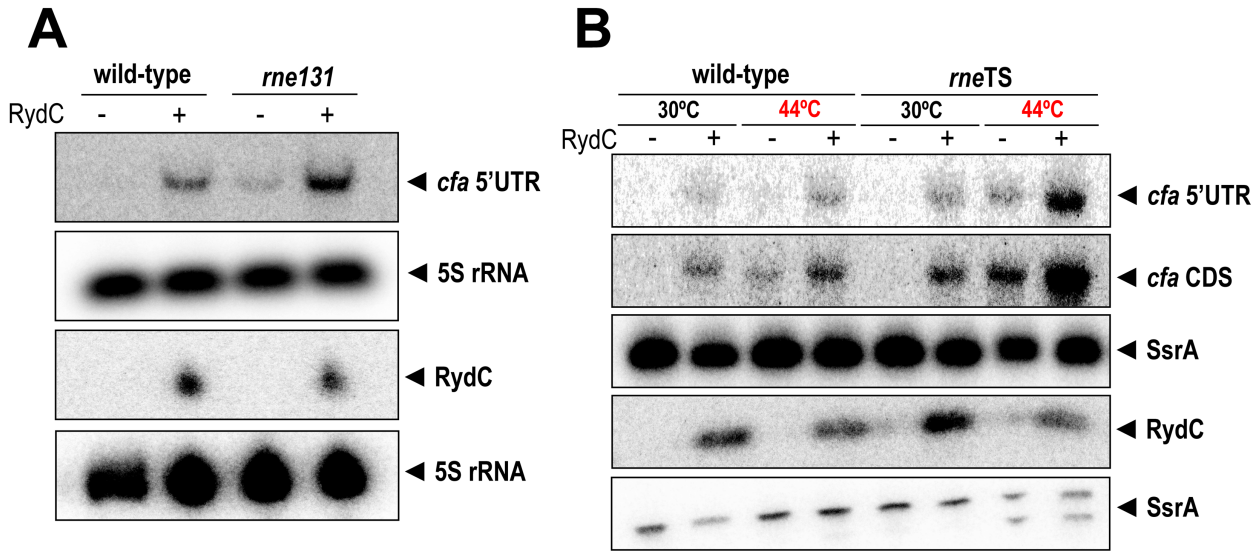

Figure 7. RydC regulates *cfa* even when RNase E is inactivated. A. Northern blot analysis was used to examine *cfa* mRNA levels in wild-type (*rne*+) and RNase E degradosome mutant (*rne131*) cells in the presence or absence of RydC. The 5S rRNA was used as an RNA loading control. **B.** Northern blot analysis was used to examine *cfa* mRNA levels in wild-type (*rne*+) and RNase E temperature-sensitive mutant (*rne*TS) cells at permissive (30°C) and non-permissive (44°C) temperatures in the presence or absence of RydC.

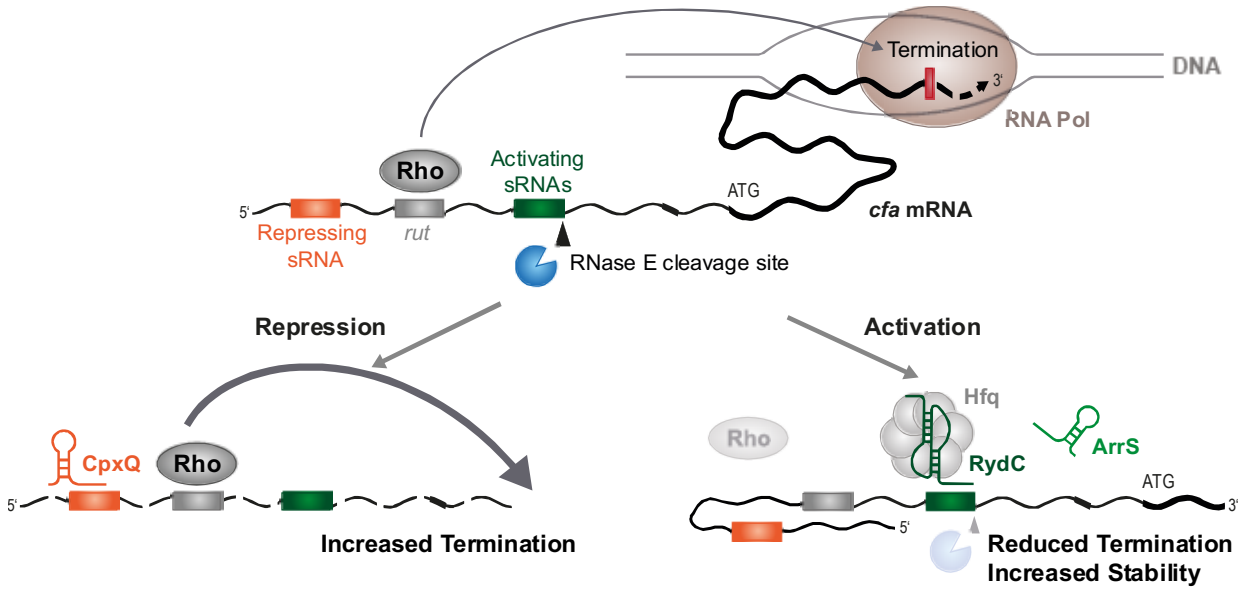

Figure 8. Model for *cfa* regulation by Rho and sRNAs. The model is described in the Discussion.